

## A comparison of nickel boride and Raney nickel electrode activity in the electrocatalytic hydrogenation of phenanthrene

BEHZAD MAHDAVI, PRZEMYSŁAW LOS, MARIE JOSÉE LESSARD, AND JEAN LESSARD<sup>1</sup>

Centre de recherche en électrochimie et électrocatalyse, Département de chimie, Université de Sherbrooke, Sherbrooke, QC J1K 2R1, Canada

Received July 14, 1994

BEHZAD MAHDAVI, PRZEMYSŁAW LOS, MARIE JOSÉE LESSARD, and JEAN LESSARD. *Can. J. Chem.* **72**, 2268 (1994).

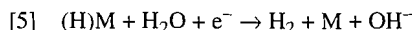
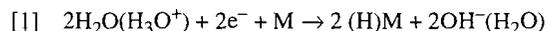
The electrocatalytic activity of nickel boride in the electrocatalytic hydrogenation (ECH) of phenanthrene in ethylene glycol – water at 80°C has been compared to that of Raney nickel and fractal nickel. The intrinsic activity of the electrode material (*real electrode activity*) is the same for nickel boride and Raney nickel electrodes and is lower for fractal nickel electrodes. The *apparent electrode activity* of nickel boride pressed powder electrodes (Ni<sub>2</sub>B electrodes) is less than that of codeposited Raney nickel (RaNi) electrodes and pressed powder fractal nickel/Raney nickel (Ni/RaNi = 50/50 to 0/100) electrodes. The apparent activity of Ni<sub>2</sub>B electrodes is improved by adding sodium chloride to the powder and dissolving it after pressing (Ni<sub>2</sub>B–NaCl electrodes). The Ni<sub>2</sub>B–NaCl electrodes have the same apparent activity as codeposited RaNi and pressed powder Ni/RaNi (20/80 to 0/100) electrodes. The apparent and real electrode activity of Ni/RaNi electrodes increases with the RaNi content up to a 20/80 ratio. The Tafel and alternating current (ac) impedance parameters were determined for the hydrogen evolution reaction (HER) in 1 M aqueous sodium hydroxide at 25°C at nickel boride and at codeposited RaNi electrodes. The intrinsic electrocatalytic activity for HER, expressed by the ratio of the exchange current density over the roughness factor ( $I_0/R$ ), is similar for Ni<sub>2</sub>B, Ni<sub>2</sub>B–NaCl, and codeposited RaNi electrodes. Surface characterization of Ni<sub>2</sub>B and Ni<sub>2</sub>B–NaCl electrodes was carried out by BET, ac impedance, scanning electron microscopy, and mercury porosimetry. No direct relation between the apparent electrode activity in ECH and the surface measured by BET and ac impedance was found. The ac impedance measurements were also carried out in the presence of sodium *trans*-cinnamate.

BEHZAD MAHDAVI, PRZEMYSŁAW LOS, MARIE JOSÉE LESSARD et JEAN LESSARD. *Can. J. Chem.* **72**, 2268 (1994).

L'activité électrocatalytique du borure de nickel est comparée à celle du nickel de Raney et du nickel fractal pour l'hydrogénation électrocatalytique (HEC) du phénanthrène dans le glycol d'éthylène – eau à 80°C. L'activité intrinsèque du matériau d'électrode (*activité réelle de l'électrode*) est la même pour le borure de nickel et le nickel de Raney et moindre pour le nickel fractal. L'*activité apparente* (activité de l'électrode) des électrodes de poudre de borure de nickel pressée (électrodes Ni<sub>2</sub>B) est moindre que celle des électrodes de nickel de Raney (RaNi) codeposé et des électrodes de poudres de nickel fractal/nickel de Raney (Ni/RaNi = 50/50 à 0/100) pressées. L'activité apparente des électrodes Ni<sub>2</sub>B est accrue par addition de chlorure de sodium à la poudre métallique puis dissolution de ce dernier après pressage (électrodes Ni<sub>2</sub>B–NaCl). Les électrodes Ni<sub>2</sub>B–NaCl ont la même activité apparente que les électrodes RaNi codeposé et les électrodes de poudre Ni/RaNi (20/80 à 0/100) pressées. L'activité apparente et l'activité réelle des électrodes Ni/RaNi croît avec la proportion de RaNi jusqu'à un rapport de 20/80. On a obtenu les paramètres de Tafel et d'impédance ac pour la réaction du dégagement d'hydrogène (RDH) en milieu hydroxyde de sodium aqueux 1 M à 25°C sur les électrodes de borure de nickel et les électrodes RaNi codeposé. L'activité électrocatalytique intrinsèque pour la RDH, exprimée par le rapport du courant d'échange sur le facteur de rugosité ( $I_0/R$ ), est sensiblement la même pour les électrodes Ni<sub>2</sub>B, Ni<sub>2</sub>B–NaCl et RaNi codeposé. La surface des électrodes Ni<sub>2</sub>B et Ni<sub>2</sub>B–NaCl est caractérisée par BET, impédance ac, microscopie électronique à balayage et porosimétrie au mercure. Il n'y a pas de relations directes entre l'activité apparente en HEC et la surface mesurée par BET et impédance ac. Les mesures d'impédance ont aussi été effectuées en présence de *trans*-cinnamate de sodium.

### Introduction

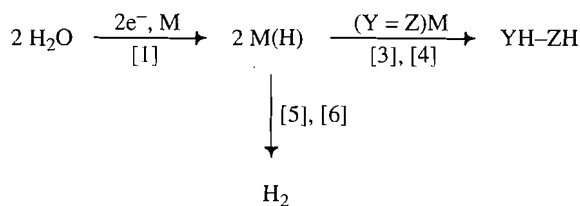
The electrocatalytic hydrogenation (ECH) of an unsaturated organic molecule in aqueous or mixed aqueous–organic media involves the mechanism described by reactions [1]–[4] where M represents the metallic surface, (H)M chemisorbed hydrogen, and (Y = Z)M the adsorbed organic substrate (1). The first step is the electroreduction of water (or hydronium ions) with the formation of adsorbed hydrogen on the electrode surface (Volmer reaction [1]), followed by reaction of the adsorbed substrate (Y = Z)M with chemisorbed hydrogen (reaction [3]). There is a competition between hydrogenation (reaction [3]) and the desorption of hydrogen by an electrochemical (Heyrovský reaction [5]) and (or) chemical (Tafel reaction [6]) pathway.



The competition between ECH and the HER may also be represented as in Scheme 1. Since, in the ECH of organic substrates, the sole processes occurring are hydrogenation and hydrogen evolution (1), the current efficiency is a measure of the competition between the two reactions. This competition depends on a number of factors such as the substrate, the reaction conditions, and the electrode (1). For a given substrate and given reaction conditions, the current efficiency for the ECH becomes, therefore, a measure of the electrode activity.

Using the ECH of phenanthrene (1) under given electrolysis conditions (see below), we have compared the activity of nickel

<sup>1</sup>Author to whom correspondence may be addressed. Telephone: (819) 821-7091. Fax: (819) 821-8017.



SCHEME 1

electrodes made of different nickel material (P-1 nickel boride, Raney nickel, and fractal nickel), and compared the activity of electrodes made of the same material but differing by the surface structure and surface area: unmodified ( $\text{Ni}_2\text{B}$ ) and modified ( $\text{Ni}_2\text{B-NaCl}$ ) nickel boride electrodes made of pressed P-1 nickel boride powder (NaCl being dissolved after pressing), codeposited Raney nickel (RaNi) electrodes (1), and pressed RaNi powder electrodes. The effect of varying the relative proportion of the fractal nickel (Ni) and RaNi on the activity of pressed Ni/RaNi electrodes was also investigated. The results reported in this paper show that the current efficiency and the conversion rate reflect the *apparent activity* of the electrode for the ECH of **1** in the specified electrolysis conditions and that the apparent activity depends on the electrode material and, for a given material, on the surface structure and surface area of the electrode as determined by mercury porosimetry, BET, and ac impedance measurements. The results also show that the ratio of the yield of the most highly hydrogenated products, octahydrophenanthrenes (octa-as **4** + octa-s **5** =  $\Sigma$  octahydrophenanthrenes) to the conversion rate, defined as coefficient  $\beta_{\text{Oct}}$ , represents the intrinsic or *real activity* of the electrode material for the ECH of **1** under the specified electrolysis conditions. The intrinsic electrocatalytic activity of  $\text{Ni}_2\text{B}$ ,  $\text{Ni}_2\text{B-NaCl}$ , and codeposited RaNi electrodes in the hydrogen evolution reaction (HER) in 1 M aqueous sodium hydroxide at 25°C, as expressed by the ratio  $I_0/R$  of the exchange current density  $I_0$  (obtained from Tafel curves) to the roughness factor  $R$  (obtained by ac impedance measurements), was also determined, together with the influence of sodium *trans*-cinnamate, a water-soluble unsaturated organic substrate, which is electrohydrogenated by ECH, on the double layer capacity of these electrodes.

## Experimental

### Electrolyses

A two-compartment glass H-cell with a jacketed cathodic compartment (volume of each compartment 25 mL) having a Nafion-324 (E.I. du Pont de Nemours & Co) membrane (1.8 cm<sup>2</sup>) as separator was connected to a Haake D8 constant temperature circulating bath filled with ethylene glycol. The counter electrode was a glassy carbon plate ( $\approx 12$  cm<sup>2</sup>) and the electrolyses were carried out with a 410 potentiostatic controller, 640 digital coulometer, and 2830 digital multimeter (Electrosynthesis Company). Phenanthrene (224  $\mu\text{mol}$ , 9 mM solution) was dissolved in a stock solution (25 mL) of sodium chloride (0.1 M) and boric acid (0.1 M) in ethylene glycol – water (24:1 v/v) by stirring and heating slightly on a hot plate. The solution was then poured into the cathodic compartment. The anodic compartment was filled with the above stock solution (25 mL) of sodium chloride and boric acid. The cathodic compartment was heated to 80°C while deaerated ( $\text{N}_2$ ), the cathode and the counter electrode were immersed and a constant current of 16 mA ( $J = 250 \text{ mA/dm}^2$ ) was applied. The cathodic solution was stirred magnetically. Aliquots (0.2 mL) were extracted with ether after the addition of a saturated NaCl solution (1 mL) and analyzed by vapour phase chromatography (vpc). The products were identified by comparison of retention times with those of authentic samples. The same system and method were used for the ECH of *trans*-

cinnamic acid (448  $\mu\text{mol}$ , 18 mM solution) in 25 mL of a 1 M aqueous solution of sodium hydroxide at room temperature. Aliquots were acidified before extraction with ether.

### Electrodes

P-1 nickel boride ( $\text{Ni}_2\text{B}$ ) was obtained by reduction of nickel acetate with sodium borohydride in an aqueous solution containing sodium hydroxide. It was prepared by following, with slight modifications, a procedure already described (2): 300 mL of an aqueous solution of sodium borohydride and sodium hydroxide was added to 1000 mL of the nickel acetate solution over a 3 h period. The product of the reaction (a black porous precipitate) was filtered on a fritted glass funnel with suction (water pump), washed with absolute ethanol, and dried at 50°C. The X-ray diffraction spectrum was identical to that reported for amorphous  $\text{Ni}_2\text{B}$  (2, 3–6). The particles had a spherical shape with an average diameter approximately equal to 0.5  $\mu\text{m}$  according to scanning electron microscopy (SEM). The electrodes were obtained by pressing the particles at  $p = 800$  or 400 MPa at room temperature. Nickel boride – sodium chloride ( $\text{Ni}_2\text{B-NaCl}$ ) electrodes were prepared in two ways. One was to first put 0.3 g of NaCl in the mold, add 1.7 or 3 g of nickel boride powder, and then put 0.3 g of NaCl on top of the nickel boride powder. The other way was to first mix 3 g of nickel boride powder with 4.5–7 g of crystalline NaCl (BDH Company), then add 0.3 g of NaCl in the mold, add the mixture of nickel boride and NaCl, and add 0.3 g of NaCl on top. The mixing of nickel boride with NaCl was made in two ways: (i) mechanical mixing of the nickel boride particles with NaCl crystals ( $\text{Ni}_2\text{B-NaCl}$ (b-solid/s)); (ii) nickel boride particles suspended in an aqueous solution of NaCl and evaporation of the water under reduced pressure ( $\text{Ni}_2\text{B-NaCl}$ (b-solution/s)). After pressing, the  $\text{Ni}_2\text{B-NaCl}$  precursory electrode was immersed for 10 min in water to completely dissolve the sodium chloride at the surface and partly dissolve (2–2.5 g) the sodium chloride within the electrode disc. The geometric surface area of the electrodes was  $2\pi \text{ cm}^2$  according to the diameter of the pressed fixed piston (2 cm). The codeposited Raney nickel electrodes consisted of Raney Ni particles dispersed in a nickel matrix, had a geometric area of 6.4 cm<sup>2</sup>, and were prepared according to the previously described method (1). The nickel/Raney nickel pressed powder ( $\text{Ni/RaNi}$ ) electrodes were prepared by pressing a mixture of fractal powder with Raney nickel alloy powder (Aldrich Company) at  $p = 800$  MPa and room temperature. The pressed powder electrodes containing RaNi were activated by leaching in 10% aqueous NaOH for 3 h at 50°C.

### Alternating current impedance measurements

Tafel and ac impedance measurements were carried out using systems and procedures analogous to those used in refs. 4 and 7–12, and using an ac amplitude of 5 mV peak-to-peak in 1 M aqueous sodium hydroxide in the absence and in the presence of *trans*-cinnamic acid, its concentration ranging from 9 to 90 mM.

## Results and discussion

The ECH of phenanthrene (**1**) at unmodified ( $\text{Ni}_2\text{B}$ ) and modified ( $\text{Ni}_2\text{B-NaCl}$ ) pressed nickel boride powder electrodes (see below), at codeposited Raney nickel (RaNi) electrodes, and at pressed fractal nickel/Raney nickel ( $\text{Ni/RaNi}$ ) electrodes was carried out on 9 mM solutions under conditions reported by Robin et al. (1) to be the best for the ECH of **1** at codeposited RaNi electrodes: ethylene glycol containing 4% of water as solvent, a slightly acidic medium containing boric acid (0.1 M) as buffer, and sodium chloride (0.1 M) as supporting electrolyte, 80°C. Two types of nickel boride electrodes were investigated: unmodified electrodes made of pressed nickel boride powder ( $\text{Ni}_2\text{B}$  electrodes), and modified electrodes made of nickel boride powder pressed with sodium chloride followed by total or partial dissolution of the sodium chloride ( $\text{Ni}_2\text{B-NaCl}$  electrodes). Electrolyses were performed under steady current control (dc) and the charge passed was 300 C (14 moles of electrons

TABLE 1. ECH of phenanthrene at nickel boride and Raney nickel electrodes at  $J = 250 \text{ mA/dm}^2$ <sup>a</sup>

Entry	Electrode <sup>b</sup>		Conversion <sup>c</sup> (%)	Yield of products <sup>c</sup> (%)			Current efficiency (%)	$\beta_{\text{oct}}^e$
	Ni <sub>2</sub> B (g)	NaCl <sup>d</sup> (g)		Di (2)	Tetra (3)	Octa (4 + 5)		
1	1.7	0	35	4	11	20	15	0.57
2	3	0 ( $p = 400 \text{ MPa}$ )	33	4	12	17	14	0.52
3 <sup>f</sup>	3	0	32–36	3–4	11–13	18–19	14–15	0.53–0.56
4 <sup>f</sup>	3 <sup>d</sup>	0.6	53–56	6	16–17	31–33	24–25	0.58–0.59
5 <sup>f</sup>	3 <sup>d</sup>	7(Solid) + 0.6	78–84	7–9	24–29	46–47	35–36	0.54–0.6
6	2 <sup>d</sup>	5(Solid) + 0.6	81	8	25	49	37	0.6
7 <sup>f</sup>	3 <sup>d</sup>	7(Solution) + 0.6	68–71	8	22–24	38–39	30–31	0.55–0.56
8 <sup>f</sup>	Codeposited RaNi electrodes <sup>g</sup>		78–85	4–6	25–35	41–49	35–37	0.51–0.62
9	Pressed RaNi electrodes <sup>h</sup>		84–86	7	29–35	42–50	35–38	0.5–0.59

<sup>a</sup>Electrolysis conditions: 224  $\mu\text{mol}$  of phenanthrene (9 mM solution); 0.1 M NaCl; 0.1 M H<sub>3</sub>BO<sub>3</sub>; T = 80°C; charged passed (Q) = 300 C (14 moles of electrons per mole of phenanthrene).

<sup>b</sup>The nickel boride electrodes were prepared by pressing the Ni<sub>2</sub>B or Ni<sub>2</sub>B–NaCl powder at  $p = 800 \text{ MPa}$  (except for entry 2).

<sup>c</sup>The conversion rate and yield of products were determined by vpc analysis. The yields are based on converted phenanthrene (material balance >99%).

<sup>d</sup>For all Ni<sub>2</sub>B–NaCl electrodes, NaCl was added both at the bottom (0.3 g) and at the top (0.3 g) of the powder layer before pressing and was dissolved afterwards by immersing electrodes in water. In entries 4, 5, and 6 the amount of NaCl mixed intimately into the Ni<sub>2</sub>B powder is indicated. "Solid" means that the Ni<sub>2</sub>B powder was mixed with crystalline NaCl. "Solution" means that the Ni<sub>2</sub>B powder was suspended in an aqueous solution of NaCl followed by the evaporation of water under reduced pressure.

<sup>e</sup> $\beta_{\text{oct}} = (4 + 5)/\text{conversion rate}$ .

<sup>f</sup>Three electrolyses were performed using three different electrodes prepared in the same way and the range of values obtained for the conversion rate, yield of products, current efficiency, and  $\beta_{\text{oct}}$  is indicated.

<sup>g</sup>See ref. 1. Geometric area: 6.4 cm<sup>2</sup>; 0.27–0.49 g of precursory alloy (48–66% in the nickel matrix).

<sup>h</sup>Prepared by pressing the Raney alloy powder at  $p = 800 \text{ MPa}$ , followed by leaching in 10% aqueous NaOH for 3 h at 50°C.

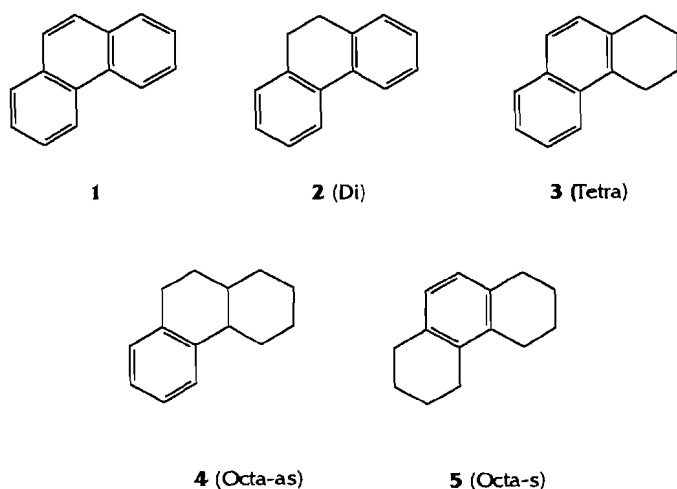


FIG. 1. The hydrogenated products of ECH of phenanthrene (1).

per mole of phenanthrene). The products formed were 9,10-dihydrophenanthrene (2), tetrahydrophenanthrene (3), and the octahydrophenanthrenes (octa-as 4 and octa-s 5) (Fig. 1). The octahydrophenanthrenes are not electrohydrogenated under the above conditions (1) and therefore the maximum current efficiency for a charge corresponding to 14 moles of electrons per mole of 1 is 57%.

#### Nickel boride electrodes

The results of entries 2 and 3 of Table 1 show that Ni<sub>2</sub>B electrodes pressed at 400 MPa (entry 2) have the same activity as electrodes pressed at 800 MPa (entry 3). A comparison of the results of entry 1 with those of entries 2 and 3 demonstrates clearly that increasing the amount of Ni<sub>2</sub>B in a Ni<sub>2</sub>B electrode by a factor 1.8 has no effect on the conversion rate and the current efficiency. This shows that the electrocatalytic hydrogenation

takes place only at the surface of the electrode disc. With the aim of increasing the active surface area of the electrode, Ni<sub>2</sub>B–NaCl electrodes were prepared by adding sodium chloride to the Ni<sub>2</sub>B powder before pressing, then removing NaCl totally or partly from the precursory electrode disc to obtain the actual electrodes (see the Experimental). Two types of Ni<sub>2</sub>B–NaCl electrodes were used: Ni<sub>2</sub>B–NaCl(s) electrodes for which NaCl was present only at the surface of the precursory electrode (see entry 4); Ni<sub>2</sub>B–NaCl(bs) electrodes for which NaCl was present both within the bulk and at the surface of the precursory electrode (see entries 5–7). It is clear from a comparison of the results of entries 4–7 with those of entries 1 and 3 that the activity of the Ni<sub>2</sub>B–NaCl electrodes is higher than that of the Ni<sub>2</sub>B electrodes, as shown by the higher conversion rates and better current efficiencies in entries 4–7. Furthermore, the activity of a Ni<sub>2</sub>B–NaCl(bs) electrode is better than that of a Ni<sub>2</sub>B–NaCl(s) electrode: higher conversion rates (78–84%) and better current efficiencies (35–37%) in entries 5 and 6 than in entry 4 (53–56% and 24–25%, respectively). However, Ni<sub>2</sub>B–NaCl(bs) electrodes are mechanically less stable than Ni<sub>2</sub>B–NaCl(s) electrodes. It was noticed that the Ni<sub>2</sub>B–NaCl(b-solution/s) electrodes prepared by suspending the Ni<sub>2</sub>B powder in a NaCl solution and evaporating water (entry 7) had a better mechanical stability than Ni<sub>2</sub>B–NaCl(b-solid/s) electrodes prepared by mixing the Ni<sub>2</sub>B powder with crystalline NaCl (entries 5 and 6), but the activity of the latter was slightly higher. Therefore, for the same amount of catalytic material and for the same geometric surface area, it is possible to increase the conversion rate and current efficiency (apparent activity of the electrode) with a simple modification in electrode design: adding sodium chloride before pressing the nickel boride powder and dissolving it afterwards. Clearly, this modification in electrode design has led to a change in surface area and (or) in surface structure that favors the ECH process over the HER. As can be seen from Table 1, the coefficient  $\beta_{\text{oct}}$  (ratio of the yield of octahydrophenanthrenes (4 + 5) to the conversion rate) determined at a

TABLE 2. ECH of phenanthrene at pressed fractal nickel/Raney Ni electrodes at  $J = 250 \text{ mA/dm}^2$ <sup>a</sup>

Entry	Electrode <sup>b</sup>		Yield of products <sup>c</sup> (%)			Current efficiency (%)	$\beta_{\text{Oct}}$ <sup>d</sup>
	Ni/RaNi (%)	Conversion <sup>e</sup> (%)	Di (2)	Tetra (3)	Octa (4 + 5)		
1	100/0	6–10	1	4–5	1–3	2–3	0.2–0.3
2	80/20	30	4	13	12	11	0.4
3	50/50	48–51	6	21–22	22–23	19–20	0.46
4	20/80	81	7–8	27–30	40–44	32–35	0.52–0.54
5	10/90	78–81	5	26–28	47	35–36	0.58–0.6
6	5/95	77	6	30	42	34	0.54
7 <sup>e</sup>	0/100	84–86	7	29–35	42–50	35–38	0.5–0.59

<sup>a</sup>See footnote a of Table 1.

<sup>b</sup>Prepared by pressing fractal nickel and Raney alloy powders at  $p = 800 \text{ MPa}$ , then leaching in 10% aqueous NaOH for 3 h at 50°C. The Ni/RaNi ratio refers to the weight ratio of fractal nickel and Raney alloy before leaching.

<sup>c</sup>See footnote c of Table 1.

<sup>d</sup>See footnote e of Table 1.

<sup>e</sup>Taken from Table 1.

charge of 300 C (14 moles of electrons per mole of phenanthrene) is constant from entry 1 to entry 7 and equal to about 0.56. This ratio is thus independent of the surface area and surface structure. It depends only on the nature of the catalytic material and represents the intrinsic activity of P-1 nickel boride for the ECH of phenanthrene under the electrolysis conditions used. It can therefore be utilized to evaluate the *real activity* of any electrode material for the ECH of phenanthrene under given conditions.

#### Raney nickel electrodes

The results of the ECH of phenanthrene (1) at codeposited RaNi electrodes and at pressed powder RaNi electrodes presented in entries 8 and 9 of Table 1 show that the two types of Raney nickel electrodes have the same apparent activity. This means that they have very similar active surface requirements (see below) for the ECH of phenanthrene even though the leaching conditions are quite different. For the codeposited RaNi electrodes, leaching of the Raney alloy particles embedded in the nickel matrix was carried out in 30% aqueous NaOH for 7 h at 80°C (1) and, for the pressed powder RaNi electrodes, the pressed Raney alloy precursory electrodes were leached in 10% aqueous NaOH for 3 h at 50°C. In the pressed electrodes, it was necessary to use much milder leaching conditions in order to leach only the top layers of the disc and prevent the pressed particles from falling apart. X-ray fluorescence shows that the amount of aluminium left in the top layers of a pressed electrode is about 6% compared to 1% in a codeposited RaNi electrode. As expected, the two types of electrodes made of the same material, Raney nickel, have the same real activity, as seen from the  $\beta_{\text{Oct}}$  value (average value 0.55–0.57). Interestingly, P-1 nickel boride and Raney nickel have the same intrinsic (real) activity for the ECH of phenanthrene under the electrolysis conditions used (same average  $\beta_{\text{Oct}}$  value of 0.56, compare entries 1–7 with entries 8 and 9, respectively). The apparent activity of the Raney nickel electrodes (entries 8 and 9) is the same as that of Ni<sub>2</sub>B–NaCl(b-solid/s) electrodes (entries 5 and 6) for which NaCl crystals were both intimately mixed within the nickel boride powder and present at the surface of the disc before its dissolution (see the Experimental). From the results of Table 1,

it is clear that the apparent electrode activity for the ECH process does not depend only on the intrinsic activity of the electrode material and, therefore, a direct evaluation of the intrinsic activity of different electrode materials for the ECH of organic substrates cannot always be made from the apparent electrode activity. For instance, the nickel boride electrodes of entries 1–3 (Ni<sub>2</sub>B unmodified electrodes) are clearly less active than Raney nickel electrodes (entries 8 and 9) for the ECH of phenanthrene although both P-1 nickel boride and Raney nickel have the same intrinsic activity.

Table 2 reports on the comparison of the apparent and real activity, for the ECH of phenanthrene, of pressed fractal nickel electrodes (entry 1) and pressed Raney nickel electrodes (entry 7), and on the effect of mixing fractal nickel particles with Raney particles in various proportions on these activities (entries 2–6). Clearly, fractal nickel ( $\beta_{\text{Oct}} = 0.25$ , entry 1) is a less active electrode material (real electrode activity) than Raney nickel ( $\beta_{\text{Oct}} = 0.55$ , entry 7). As a result, the apparent activity of fractal nickel electrodes is much lower (much smaller conversion rates and current efficiencies) than that of Raney nickel electrodes. For the Ni/RaNi electrodes (entries 2–6), as the proportion of Raney nickel is increased (decreasing Ni/RaNi ratio), the real activity and thus the apparent activity increase until the proportion of RaNi reaches 80% (entry 4). At this point, the Ni/RaNi (20/80) electrodes have the same activity (real and apparent) as the 100% RaNi electrodes (entry 7). The activity for ECH is related to the competition between hydrogenation (eq. [3]) and hydrogen evolution (eq. [4] and (or) [5]), as already mentioned (see Scheme 1 also), and for a Ni/RaNi ratio of 20/80 the influence of Ni is too small to be detected within the experimental error. The ECH of phenanthrene on Ni/RaNi electrodes confirms that  $\beta_{\text{Oct}}$  does reflect the activity of the catalytic material, since the  $\beta_{\text{Oct}}$  value varies between that of a 100% fractal Ni electrode and that of a 100% RaNi electrode as the Ni/RaNi ratio decreases.

#### Tafel and alternating current impedance parameters for the HER in alkaline medium

To characterize further the pressed nickel boride powder and codeposited Raney nickel electrodes used above in the ECH of

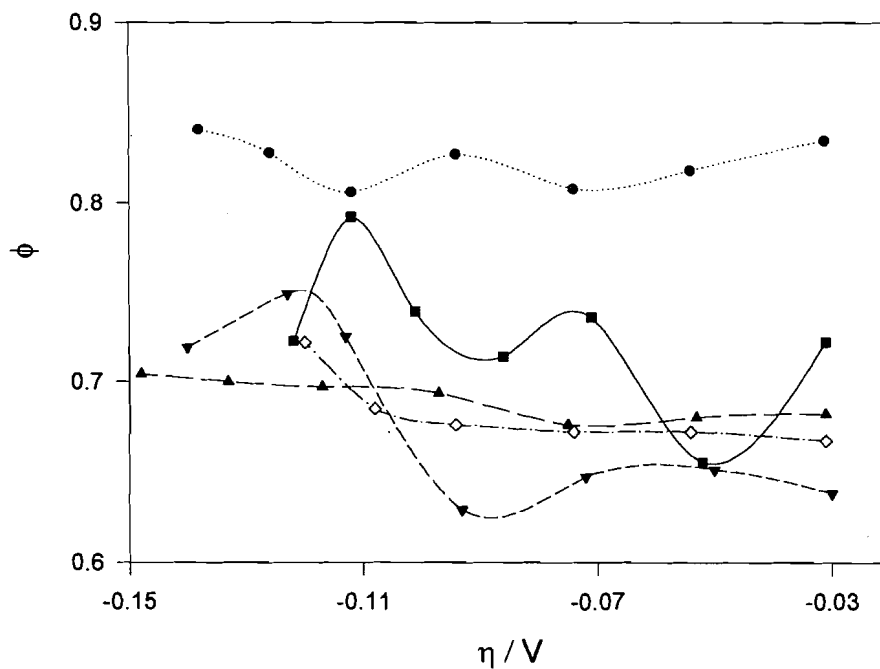


FIG. 2. Constant phase angle as a function of the overpotential for pressed nickel boride powder electrodes in 1 M NaOH at 25°C: (●) Ni<sub>2</sub>B; (■) Ni<sub>2</sub>B-NaCl(s); (▼) Ni<sub>2</sub>B-NaCl(b-solid/s); (▲) Ni<sub>2</sub>B-NaCl(b-solution/s); (◇) Ni<sub>2</sub>B ( $p = 400$  MPa).

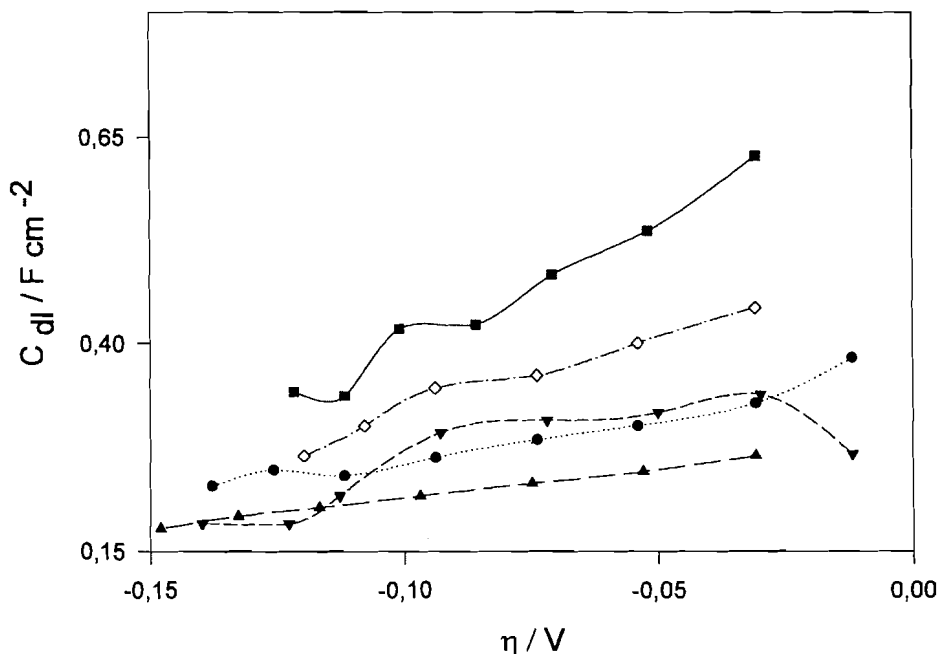


FIG. 3. Double layer capacities as a function of the overpotential for pressed nickel boride powder electrodes in 1 M NaOH at 25°C: (●) Ni<sub>2</sub>B; (■) Ni<sub>2</sub>B-NaCl(s); (▼) Ni<sub>2</sub>B-NaCl(b-solid/s); (▲) Ni<sub>2</sub>B-NaCl(b-solution/s); (◇) Ni<sub>2</sub>B ( $p = 400$  MPa).

phenanthrene, we determined their intrinsic activity and their real surface for the HER in 1 M NaOH at 25°C using Tafel plots and ac impedance measurements (4, 7–12). Such studies could not be carried out on the pressed RaNi electrodes because of the continuous leaching of the Raney alloy particles inside the disc during the experiments, causing the particles to fall apart. For the determination of the double layer capacity ( $C_{dl}$ ) by ac impedance, the CPE model was used (eqs. [7] and [8] (13) where  $\omega$  is the angular frequency of the ac signal,  $T$  is a constant,  $\phi$  is the phase angle related to the surface roughness,  $R_s$  is the solution resistance, and parameter  $A$  is equal to  $1/R_{ct}$  where

$R_{ct}$  is the charge transfer resistance (4, 7–12, 14)). For an ideally flat electrode,  $\phi$  is equal to 1 and thus  $T$  is equal to  $C_{dl}$ . The roughness factor  $R$  was estimated from the experimental values of the capacity of the double layer divided by  $27.9 \mu\text{F}/\text{cm}^2$ , the capacity of a platinum smooth surface (15).

$$[7] \quad Z_{CPE} = 1/T(j\omega)^\phi$$

$$[8] \quad T = C_{dl}^\phi (R_s^{-1} + A)^{(1-\phi)}$$

Figure 2 shows the dependency of  $\phi$  on the overpotential ( $\eta$ )

TABLE 3. Tafel parameters, roughness factors, and real current densities for the HER in 1 M NaOH at 25°C

Entry	Electrode <sup>a</sup> (3 g of Ni <sub>2</sub> B)		$I_0$ (mA cm <sup>-1</sup> )	$b$ (mV)	o.c.p. <sup>c</sup> (mV)	$r^2$	$\eta_{150}$ (mV)	$C_{dl}^d$ (F cm <sup>-2</sup> )	$R$	$I_0/R^e$ (A cm <sup>-2</sup> )
	NaCl <sup>b</sup> (g)									
1	0		2.8	106	-30	0.999	183	0.28	10 000	$2.8 \times 10^{-7}$
2	0 ( $p = 400$ MPa)		3.4	108	-30	0.997	182	0.25	9 000	$3.8 \times 10^{-7}$
3	0.6		3.7	102	-30	0.996	165	0.48	17 400	$2.1 \times 10^{-7}$
4	7(Solid) + 0.6		3.4	127	0	0.995	205	0.25	9 000	$3.8 \times 10^{-7}$
5	7(Solution) + 0.6		2.6	118	0	0.998	207	0.22	7 900	$3.3 \times 10^{-7}$
6	Codeposited RaNi electrodes		7.3	123	0	0.992	175	0.55	20 000	$3.7 \times 10^{-7}$

<sup>a</sup>The nickel boride electrodes were prepared by pressing the Ni<sub>2</sub>B or Ni<sub>2</sub>B-NaCl powder at  $p = 800$  MPa (except in entry 2).

<sup>b</sup>See footnote *d* of Table 1.

<sup>c</sup>Open circuit potential obtained from extrapolation of the low-current part of the Tafel curves to zero current.

<sup>d</sup>Mean values obtained from the experimental  $C_{dl}$  values measured at different overpotentials (see Fig. 3).

<sup>e</sup>Real current density.

for different nickel boride electrodes. The  $\phi$  value is the highest (0.83) for an electrode of Ni<sub>2</sub>B powder pressed at 800 MPa. It is smaller for an electrode of Ni<sub>2</sub>B powder pressed at 400 MPa ( $\phi = 0.68$ ) and also for the Ni<sub>2</sub>B-NaCl electrodes ( $\phi = 0.65$ – $0.75$ ). Thus, the latter electrodes behave more like the limiting case of a true porous electrode for which  $\phi$  is equal to 0.5 (11). The mean  $\phi$  value for a codeposited RaNi electrode is 0.75. In Fig. 3, the decrease of  $C_{dl}$  with  $\eta$  for the various nickel boride electrodes used in Table 1 is shown. For the codeposited RaNi electrodes  $C_{dl}$  also decreases with  $\eta$  (16). This decrease is due to hydrogen bubbles formed on the surface (17). The roughness factors  $R$  presented in Table 3 were estimated from the mean value of the experimental  $C_{dl}$  values measured at the different overpotentials (see Fig. 3). The codeposited RaNi electrodes have the highest  $R$  value and the various nickel boride electrodes have different  $R$  values. This will be discussed below (see *Surface studies*).

Based on the overpotential at 150 mA/cm<sup>2</sup> ( $\eta_{150}$ ), the electrocatalytic activity of the nickel boride and codeposited RaNi electrodes for the HER in 1 M aqueous NaOH at 25°C decreases in the order: Ni<sub>2</sub>B-NaCl(s) ( $\eta_{150} = 165$  mV, entry 3) > codeposited RaNi ( $\eta_{150} = 175$  mV, entry 6) > Ni<sub>2</sub>B (unmodified) ( $\eta_{150} = 182$ – $183$  mV, entries 1 and 2) > Ni<sub>2</sub>B-NaCl(bs) ( $\eta_{150} = 203$ – $207$  mV, entries 4 and 5). The decreasing order of apparent activity of these same electrodes for the ECH of phenanthrene in ethylene glycol at 80°C and pH 3–6 (see discussion above and Table 1) is as follows: codeposited RaNi (entry 8) ~ Ni<sub>2</sub>B-NaCl(b-solid/s) (entries 5 and 6) > Ni<sub>2</sub>B-NaCl(b-solution/s) (entry 7) > Ni<sub>2</sub>B-NaCl(s) (entry 4) > Ni<sub>2</sub>B (unmodified) (entries 1–3). Therefore there is no direct relation between the electrode activity in the ECH of phenanthrene under the conditions used and the electrode activity for the HER in aqueous alkali. It was likewise found that for RaNi and RaNiXY (XY = CoCr, CrMo, CrTi, CuCr, CuTi, and CrTi) electrodes, there was no direct relation between the activity of the electrodes in the two electrolytic processes: the most active electrode for the ECH of phenanthrene was the RaNi electrode, which was less active than the RaNiXY electrodes for the HER in alkaline solution.<sup>2</sup> Interestingly, the intrinsic electrocatalytic activity for the HER, expressed by the ratio of the exchange current density over the roughness factor ( $I_0/R$ ), is of a similar order of magnitude ( $(2$ – $4) \times 10^{-7}$ ) for all the electrodes of Table 3 just as the real electrode activity of these same electrodes for the ECH of phenanthrene

TABLE 4. Specific surface area and diameter of pores for selected nickel boride electrodes

Entry	Electrode <sup>a</sup> (3 g of Ni <sub>2</sub> B)		Specific surface area <sup>c</sup> (m <sup>2</sup> /g)	$R^d$	Pore diameter <sup>e</sup> ( $\mu$ m)
	NaCl <sup>b</sup> (g)				
1	0		10.7	10 000	0.012
2	0.6		9.7	17 400	0.012
3	7(Solid) + 0.6		9	9 000	8

<sup>a</sup>See footnote *b* of Table 1.

<sup>b</sup>See footnote *d* of Table 1.

<sup>c</sup>Obtained from BET measurements and based on the mass of Ni<sub>2</sub>B for Ni<sub>2</sub>B-NaCl electrodes.

<sup>d</sup>Taken from Table 3, entries 1, 3, and 4.

<sup>e</sup>Obtained from mercury porosimetry measurements.

was the same (average  $\beta_{oct}$  value of 0.55–0.57, Table 1). This shows that the intrinsic activity for the HER is determined by the electrode material and not by the surface structure and the real surface area, as is the real activity in the ECH of phenanthrene (see above). It is coincidental that two different electrode materials, nickel boride and Raney nickel, give the same real electrode activity for the ECH of phenanthrene. For instance, RaNiXY electrodes have a lower real activity for the ECH of phenanthrene than RaNi electrodes.<sup>2</sup>

Two of the electrodes of Table 3, the Ni<sub>2</sub>B (unmodified) (entries 1 and 2) and Ni<sub>2</sub>B-NaCl(s) (entry 3) electrodes, have a negative ( $-30$  mV) open circuit potential (o.c.p.) (obtained by extrapolating the low-current part of the Tafel curve to zero current) while the three others (entries 4–6) have an o.c.p. of 0 mV. A negative o.c.p. has been attributed to hydrogen absorption to form metal hydrides (4, 18).

#### Electrocatalytic activity and surface of nickel boride electrodes

We have shown above (see *Nickel boride electrodes*) that modifying the nickel boride electrodes made of pressed powder, by adding NaCl before pressing and dissolving it afterwards, caused an increase of the apparent activity for the ECH of phenanthrene (Table 1), and suggested that their improved activity was related to a change in surface area and (or) structure. To clarify this point, surface studies were carried out on nickel boride electrodes having different apparent activities for the ECH of phenanthrene by determination of the specific surface area using the BET method, by scanning electron microscopy (SEM), and by pore size measurements using mercury

<sup>2</sup>J.M. Chapuzet, J. Depo, G.A. Capuano, and J. Lessard. Unpublished results.

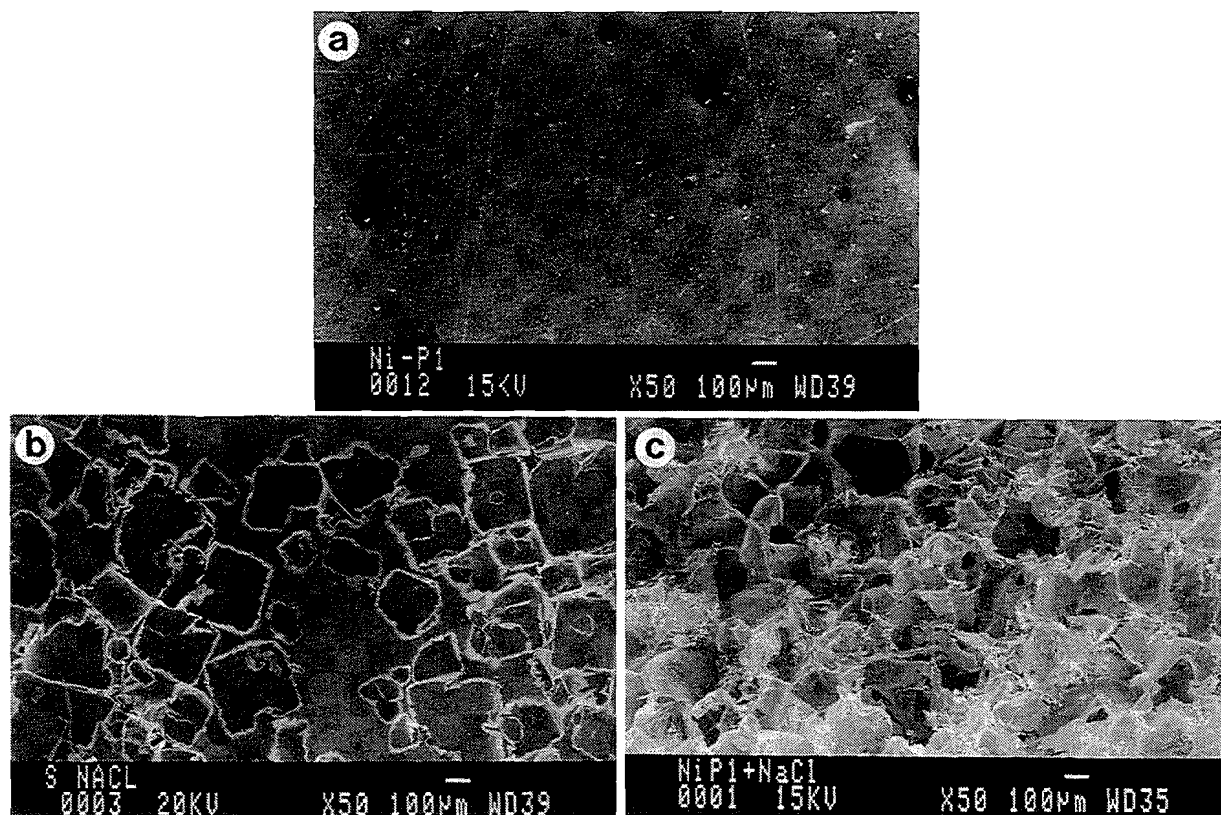


FIG. 4. SEM pictures of pressed nickel boride powder electrodes after removing NaCl: (a)  $\text{Ni}_2\text{B}$ ; (b)  $\text{Ni}_2\text{B-NaCl(s)}$ ; (c)  $\text{Ni}_2\text{B-NaCl(b-solid/s)}$ .

porosimetry. The data for  $\text{Ni}_2\text{B}$ ,  $\text{Ni}_2\text{B-NaCl(s)}$ , and  $\text{Ni}_2\text{B-NaCl(b-solid/s)}$  electrodes (order of increasing apparent activity) are collected in Table 4 (entries 1–3, respectively) together with the roughness factor ( $R$ ) for the HER in alkaline medium. The SEM pictures are shown in Fig. 4.

The specific surface area of the pressed  $\text{Ni}_2\text{B}$  powder (entry 1) is exactly the same as that of the free powder ( $10 \text{ m}^2/\text{g}$ ), which means that pressing did not remove any site accessible to the nitrogen molecules. The specific surface area decreases slightly from the least active  $\text{Ni}_2\text{B}$  electrode (entry 1) to the most active  $\text{Ni}_2\text{B-NaCl(b-solid/s)}$  electrode (entry 3). So there is no direct correlation between the permeability to nitrogen molecules and the apparent activity for the ECH of phenanthrene. There is no direct correlation between the specific surface area and either the roughness factor or the electrocatalytic activity based on  $\eta_{150}$  for the HER in alkaline medium: the  $\text{Ni}_2\text{B}$  electrode with the largest specific surface area (entry 1) does not have the largest roughness factor and the highest electrocatalytic activity. One possible cause for the lack of correlation between the specific surface area and the activity in the electrocatalytic processes studied could be the difference in the nature of the interface: a gas–solid interface in the BET measurements and a solution–solid interface in the ECH process and the HER. Furthermore, the solid is polarized in the electrochemical processes. When comparing the two electrocatalytic processes, there is no direct correlation between the apparent electrode activity for the ECH process and the electrode activity for the HER, as already pointed out. The latter activity refers to the overpotential for the HER in aqueous alkali and the overpotential is determined by the rate of the slow step, which is the electrochemical desorption of chemisorbed hydrogen (Heyrovský step [5]) on nickel boride electrodes (4). The apparent

activity for the ECH process refers to the competition between the hydrogenation step [3] and desorption of chemisorbed hydrogen (eqs. [5] and (or) [6]), that is, on the relative rates of reaction [3] and reactions [5] and (or) [6]. Since the hydrogenation step involves the reaction between the adsorbed organic substrate and chemisorbed hydrogen, accessibility of the sites for the adsorption of the former (mass transfer to the active sites) is bound to play a role in the ECH reaction (see below). Thus the surface requirements for the ECH reaction are expected to differ from those of the HER in which only chemisorbed hydrogen is involved. Therefore the most active electrode in the ECH process (the  $\text{Ni}_2\text{B-NaCl(s-solid/s)}$  electrode in this case) does not necessarily have to be the most active electrode in the HER under different electrolysis conditions, as experimentally found (the  $\text{Ni}_2\text{B-NaCl(s)}$  electrode is the most active in the HER).

There is good agreement between the SEM pictures (Fig. 4) and the size of the pores determined by mercury porosimetry. The  $\text{Ni}_2\text{B}$  and  $\text{Ni}_2\text{B-NaCl(s)}$  electrodes have pores of the same size (diameter of  $0.012 \mu\text{m}$ , Table 4, entries 1 and 2) and appear to have the same compactness on the SEM pictures (Figs. 4a and 4b, respectively). In Fig. 4b, the prints left by the NaCl crystals after their dissolution are clearly seen and the surface in contact with solution should be larger in the case of the  $\text{Ni}_2\text{B-NaCl(s)}$  electrodes, and, indeed, the roughness factor of the latter electrode is larger (17 400 in entry 2 compared to 10 000 in entry 1 for the  $\text{Ni}_2\text{B}$  electrode). As result, the  $\text{Ni}_2\text{B-NaCl(s)}$  electrode is more active both for the ECH of phenanthrene (compare entry 4 with entries 1–3 of Table 1) and the HER in alkaline medium (lower  $\eta_{150}$  in entry 3 than in entries 1 and 2 of Table 3). The  $\text{Ni}_2\text{B-NaCl(b-solid/s)}$  electrodes resulting from intimate mixing of NaCl crystals within the nickel boride pow-

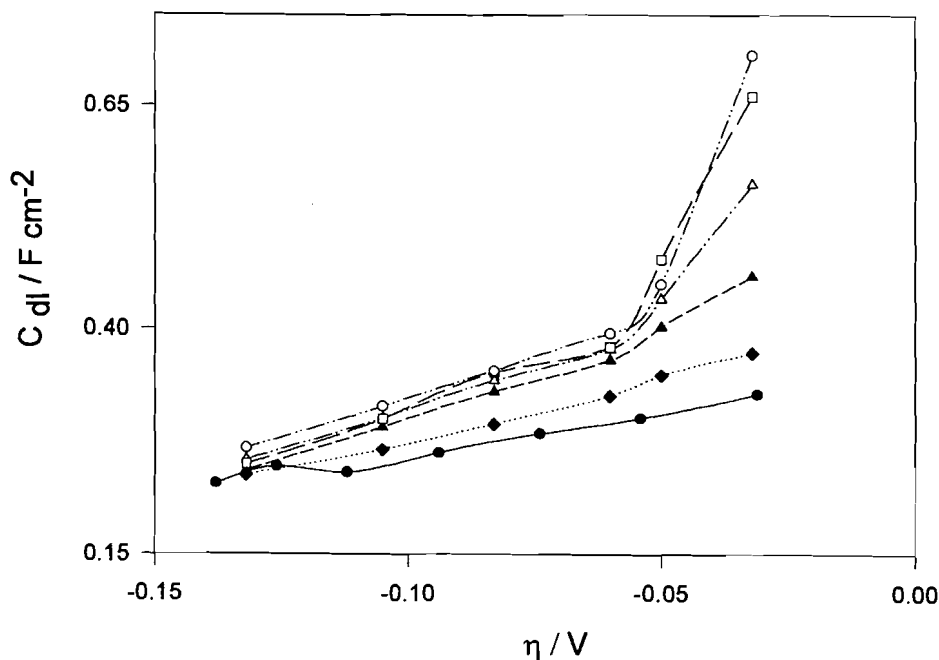


Fig. 5. Double layer capacities as a function of the overpotential and the *trans*-cinnamic acid concentration for a  $\text{Ni}_2\text{B}$  electrode in 1 M NaOH at 25°C: (●)  $C = 0$  mM; (◆)  $C = 9$  mM; (▲)  $C = 27$  mM; (△)  $C = 45$  mM; (□)  $C = 72$  mM; (○)  $C = 90$  mM.

der plus the addition of NaCl at the surface have much larger pores (Table 4, entry 3) than the two other electrodes (entries 1 and 2) and also appear quite different (much rougher) on the SEM picture (compare Fig. 4c with Figs. 4a and 4b). Surprisingly, the  $\text{Ni}_2\text{B}$ -NaCl(b-solid/s) electrode has also the same roughness factor ( $R = 9000$ ) as a  $\text{Ni}_2\text{B}$  electrode ( $R = 9000$ – $10\,000$ ) and is the least active (has the highest  $\eta_{150}$ ) of the three electrodes of Table 3 for the HER. Thus, the solution–solid interface and the number of sites for the chemisorption of hydrogen are not increased in the less closely packed structure of a  $\text{Ni}_2\text{B}$ -NaCl(b-solid/s) electrode. However, the  $\text{Ni}_2\text{B}$ -NaCl(b-solid/s) electrode has the highest apparent activity of the three electrodes of Table 3 for the ECH of phenanthrene and this could be explained by a larger number of readily accessible sites for the adsorption of phenanthrene (ECH active sites) due to the larger pores. For probing the existence of more readily accessible adsorption sites for the organic substrate in the  $\text{Ni}_2\text{B}$ -NaCl(b-solid/s) electrode, we carried out ac impedance measurements on  $\text{Ni}_2\text{B}$  and  $\text{Ni}_2\text{B}$ -NaCl(b-solid/s) electrodes in the presence of sodium *trans*-cinnamate in 1 M NaOH at 25°C, after the work of Kam Cheong et al. (16). They found that  $C_{dl}$  of codeposited Raney electrodes in 1 M KOH at 25°C is increased in the presence of potassium *trans*-cinnamate, a water-soluble substrate that is electrohydrogenated by ECH, and attributed this increase to its adsorption on the electrode. According to their hypothesis, for a given concentration of sodium *trans*-cinnamate, the increase of  $C_{dl}$  should be more pronounced for an electrode having sites that are more readily accessible for the adsorption and hydrogenation of the organic substrate. And in agreement with this hypothesis, the maximum  $C_{dl}$  value at low overpotential ( $> -0.05$  V, close to the o.c.p. obtained from the Tafel curves) (see Figs. 5 and 6) is reached at a lower concentration of sodium *trans*-cinnamate ( $C = 27$  mM, Fig. 6) on a less closely packed  $\text{Ni}_2\text{B}$ -NaCl(b-solid/s) electrode, which should have more readily accessible sites for adsorption and hydrogenation of the organic substrate, than on a  $\text{Ni}_2\text{B}$  electrode ( $C = 90$  mM, Fig. 5). The higher apparent activity of the former electrode would then be related to the accessibility of the ECH

active sites and thus to the efficiency of the mass transfer of the organic substrate to these sites. It is interesting to note in Figs. 5 and 6 that the increase of  $C_{dl}$  with the concentration of sodium *trans*-cinnamate occurs only at low overpotentials. At these low overpotentials, the current density is about the same as that used for the ECH electrolyses. At higher overpotentials ( $\eta < -0.1$  V), the HER predominates and bubbles of hydrogen cover the surface of the electrode; the presence and concentration of *trans*-cinnamate have little effect on  $C_{dl}$ . This suggests that at these potentials there is little adsorption of the organic substrate on the electrode surface because an effective mass transfer to the active sites is prevented by the bubbles of hydrogen covering the surface and (or) because at more cathodic potentials there is desorption of sodium *trans*-cinnamate. We emphasize the fact that a  $\text{Ni}_2\text{B}$ -NaCl(b-solid/s) electrode, which is more active than a  $\text{Ni}_2\text{B}$  electrode for the ECH of phenanthrene in ethylene glycol – water containing  $\text{H}_3\text{BO}_3$  at 80°C (see Table 1), is also more active for the ECH of sodium *trans*-cinnamate in 1 M aqueous NaOH at 25°C as shown by the higher current efficiency and conversion rate in entry 2 of Table 5 than those in entry 1. Thus the electrodes show the same behaviour in these two ECH reactions despite the different conditions.

### Conclusion

We have shown in this paper that the apparent electrode activity for the ECH of phenanthrene (as measured by the conversion rate, the yield of octahydrophenanthrenes, and the current efficiency) of nickel boride electrodes is increased by pressing the P-1 nickel boride powder with NaCl and dissolving it afterwards. This increase of activity does not correspond to an increase in the specific surface area measured by the BET method and does not correlate directly either with the roughness factor (obtained from ac impedance measurements on the HER in aqueous alkaline medium) or with the electrocatalytic activity for the HER in aqueous alkaline medium (based on the  $\eta_{150}$  value determined from Tafel curves). The fact that the increase of  $C_{dl}$  with the concentration of sodium *trans*-cinnamate, which is electrohydrogenated to sodium 3-phenylpropanoate in aque-

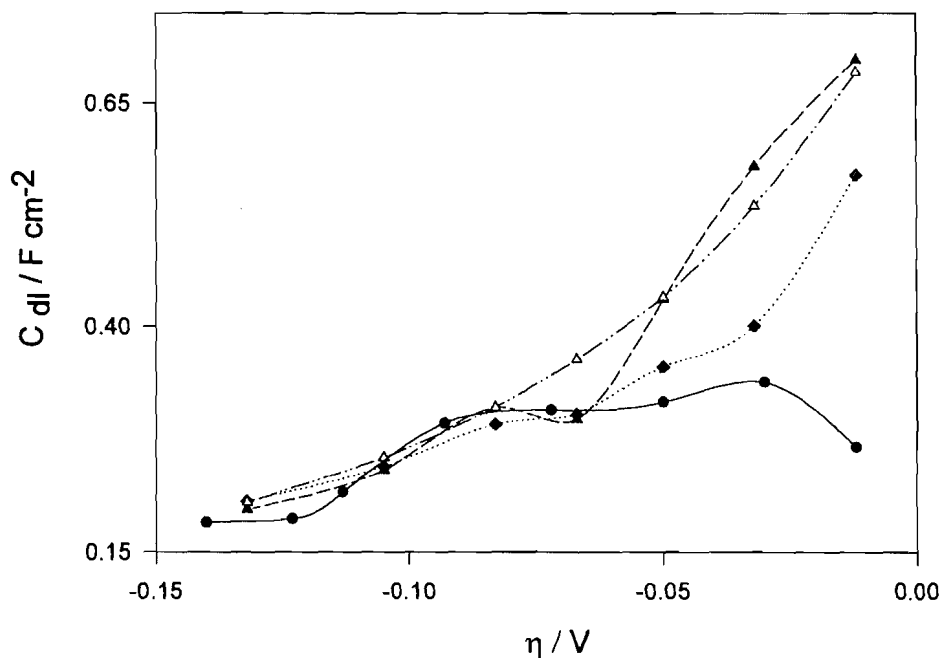


FIG. 6. Double layer capacities as a function of the overpotential and the *trans*-cinnamic acid concentration for a Ni<sub>2</sub>B-NaCl(b-solid/s) electrode in 1 M NaOH at 25°C: (●) *C* = 0 mM; (◆) *C* = 9 mM; (△) *C* = 27 mM; (▲) *C* = 72 mM.

TABLE 5. ECH of *trans*-cinnamic acid at nickel boride electrodes at *J* = 250 mA/dm<sup>2a</sup>

Entry	Electrode <sup>b</sup> (3 g of Ni <sub>2</sub> B)	Yield of hydrocinnamic acid <sup>c</sup> (%)	Current efficiency (%)
	NaCl <sup>d</sup> (g)		
1	0	21	21
2	7(Solid) + 0.6	42	42

<sup>a</sup>Electrolysis conditions: 448 μmol of *trans*-cinnamic acid (18 mM solution); 1 M NaOH; T = 25°C; charged passed (*Q*) = 88 C (2 moles of electrons per mole of *trans*-cinnamic acid).

<sup>b</sup>See footnote *b* of Table 1.

<sup>c</sup>The yield of product and conversion rate were similar (material balance >96%) and were determined by vpc analysis.

<sup>d</sup>See footnote *d* of Table 1.

ous alkaline medium, was steeper (maximum  $C_{dl}$  reached at lower concentrations of cinnamate) for a more active electrode together with the pore size effect (larger pore diameter for the most active electrode as determined by mercury porosimetry and as confirmed by SEM) led to the conclusion that the apparent activity for the ECH of phenanthrene depends not only on the true area of the solution–solid interface but also the accessibility of the active sites, that is, on the mass transfer of the organic substrate to the active sites.

The ratio of the yield of octahydrophenanthrenes to the conversion rate (defined as  $\beta_{occl}$ ) was found to be independent of the true area of the solution–solid interface and the accessibility of the active sites since it is the same for all the nickel boride electrodes (modified and unmodified) investigated. It depends only on the electrode material and thus must represent the true or real electrode activity for the ECH of phenanthrene under given conditions. Similarly, the intrinsic activity for the HER in alkaline medium as measured by the ratio of exchange current den-

sity to the roughness factor ( $I_0/R$ ) is the same for all nickel boride electrodes studied. It is noteworthy that nickel boride and Raney nickel electrodes have the same real activity for the ECH of phenanthrene and the same intrinsic activity for the HER in basic aqueous medium. Fractal nickel is much less active than Raney nickel as electrode material (real activity and apparent activity) for the ECH of phenanthrene and the activity of Ni/RaNi electrodes increases with the RaNi content up to a 20/80 ratio. With 20% of less fractal nickel, its influence on the activity of Ni/RaNi electrodes is not detected within the experimental errors.

#### Acknowledgements

Financial support from the Natural Sciences and Engineering Research Council of Canada, the "Fonds pour la formation de chercheurs et l'aide à la recherche du Québec", and the "Ministère de l'énergie et des ressources du Québec" is gratefully acknowledged. We thank Sylvain Roy for mercury porosimetry measurements.

1. D. Robin, M. Comtois, A. Martel, R. Lemieux, A. Kam Cheong, G. Belot, and J. Lessard. *Can. J. Chem.* **68**, 1218 (1990).
2. C.A. Brown. *J. Org. Chem.* **35**, 1900 (1970).
3. J. Saida, A. Inone, and T. Masumoto. *Metall. Trans. A*: **22**, 2125 (1992).
4. P. Los and A. Lasia. *J. Electroanal. Chem.* **333**, 115 (1992).
5. J. van Wouterghem, S. Morup, Ch.J. Koch, S.W. Charles, and S. Wells. *Nature*, **322**, 622 (1986).
6. M.L. Trudeau, J.Y. Huot, R. Schulz, D. Dussault, A. van Neste, and G. L'Esperance. *Phys. Rev. B*, **45**, 4626 (1992).
7. E. Potvin, A. Lasia, H. Ménard, and L. Brossard. *J. Electrochem. Soc.* **138**, 900 (1991).
8. L. Chen and A. Lasia. *J. Electrochem. Soc.* **138**, 3321 (1991).
9. Y. Choquette, L. Brossard, A. Lasia, and H. Ménard. *Electrochim. Acta*, **35**, 1251 (1990).
10. P. Los, A. Rami and A. Lasia. *J. Appl. Electrochem.* **23**, 135 (1993).
11. P. Los, A. Lasia, L. Brossard, and H. Ménard. *J. Electroanal. Chem.* **360**, 101 (1993).

12. P. Los, L. Brossard, H. Dumont, A. Lasia, J. Lessard, and H. Ménard. Proceedings of the 5th Canadian Hydrogen Workshop, Ottawa, February 1992. p. 39.
13. G.J. Brug, A.L.G. van den Eeden, M. Sluyters-Rehbach, and J.H. Sluyters. *J. Electroanal. Chem.* **176**, 275 (1984).
14. D.A. Harrington and B.E. Conway. *Electrochim. Acta*, **32**, 1703 (1987).
15. L. Bai, L. Goa, and B.E. Conway. *J. Chem. Soc. Faraday Trans.* **89**, 235 (1993).
16. A. Kam Cheong, A. Lasia, and J. Lessard. *J. Electrochem. Soc.* **141**, 975 (1994).
17. A. Rami and A. Lasia. *J. Appl. Electrochem.* **22**, 376 (1992).
18. D.M. Soares, O. Teschke, and I. Torriani. *J. Electrochem. Soc.* **139**, 98 (1992).